rived from the mRNAs of wild-type and targeted SK3 alleles permitted quantification of the relative contribution by the two alleles. One-third of the PCR was prepared as a Southern blot, probed with a mixture of β-actin and SK3 oligonucleotides, and imaged on a PhosphorImager 445SI; signals were quantified with IP Lab Gel software (molecular Dynamics, Sunnyvale, CA). Data from individual animals were obtained in two to seven experiments, normalized to β-actin, standardized across experiments, and averaged to give one value per animal. These values were pooled according to genotype and drug treatment. For Northern blots, the total RNA was electrophoresed through a 1.4% agarose containing 1.0 M formaldehyde, blotted on nylon membranes, and probed for mouse SK3. A single SK3 mRNA, 10 kb, is detected in all mouse tissues, although two bands are detected in rat tissues (*3, 10*). Blots were stripped and reprobed for 18*S* rRNA. For Western blots, snap-frozen tissue was pulverized under liquid nitrogen, hand-dounced in ice-cold sucrose (320 mM) with mammalian protease inhibitor cocktail (Sigma), and microfuged at 10,000*g* for 10 min at 4°C; the supernatant was centrifuged at 100,000*g* at 4°C for 60 min. The membrane pellet was resuspended in sucrose with mammalian protease inhibitor cocktail and sonicated for 10 s. Western blots (20 μg) were prepared and probed with antibody to SK3 (1:1000) or antibody to Na^+- and K^+-dependent adenosine triphosphatase (Na^+,K^+-ATPase) (1:50,000) (gift of S. Luchenko). Following secondary antibody (goat antirabbit immunoglobulin G–horseradish peroxidase), immunoreactivity was detected with Super Signal West Pico Chemiluminescent Substrate and X-Omat Blue XB-1 film.

7. C. T. Bond, J. Maylie, J. P. Adelman, unpublished observation.
8. A polyclonal antiserum directed against SK3 protein was raised in rabbits using the immunogenic peptide ADTLRQQQQQLLTAFVEAR, synthesized on a Lys^8 core linked to a solid-phase peptide synthesis support (A, Ala; D, Asp; E, Glu; F, Phe; L, Leu; Q, Gln; R, Arg; T, Thr; and V, Val). Antibodies were used for all immunohistochemistry experiments and the Western blot presented in Fig. 2. SK3 immunoreactivity was localized with an avidin-biotin peroxidase method with 40-μm free-floating cryostat sections. Antibody was applied at a dilution of 1:80,000.
9. W. A. Kaufmann *et al.*, *Eur. J. Neurosci.* **10**, 1084 (1998).
10. D. Pribnow *et al.*, *Muscle Nerve* **22**, 742 (1999).
11. Cultured myotubes were prepared from the hindlimb muscles of postnatal day 2 mice (*30*). Whole-cell patch clamp recordings were performed on multinucleated myotubes 6 to 9 days after plating. Culture dishes were perfused with oxygenated Tyrode solution (140 mM NaCl, 5 mM KCl, 1 mM $MgCl_2$, 10 mM dextrose, 10 mM Hepes, and 1.8 mM $CaCl_2$) with pH of 7.35. Patch electrodes (2 to 4 megohms) were filled with internal solution (105 mM K^+ aspartate, 10 mM NaCl, 10 mM Hepes, 40 mM KCl, 1 mM $MgCl_2$, 0.05 mM EGTA, and 5 mM Mg–adenosine 5′-triphosphate) with pH of 7.10. Nearly all cells visibly contracted during voltage steps or ramps. Statistical significance was determined post hoc by analysis of variance (ANOVA) and Bonferroni tests.
12. T. Tanabe, K. G. Beam, B. A. Adams, T. Niidome, S. Numa, *Nature* **346**, 569 (1990).
13. Baseline respiratory pattern and the response to hypoxia (8% oxygen for 5 min at 30°C) were measured in a body plethysmograph. Individual unanesthetized animals were placed in a 65-ml chamber with their head exposed. A pneumotachograph was connected to the chamber and to a differential pressure transducer. The analog signal from the transducer was amplified, converted to digital, displayed on a monitor, and stored to disk by computer for later analysis. Results are expressed as a percentage of the baseline respiratory rate determined during 5 min before the hypoxia. In separate studies of respiratory timing, inspiratory time, expiratory time, respiratory cycle duration, and the fraction of the respiratory cycle duration occupied by the inspiratory time were determined by analyzing 50 consecutive breaths for a representative period of 15 min in air. Data are expressed as mean ± SD, and differences between groups were examined with one-way ANOVA followed by the Newman-Keuls test.
14. J. P. Mortola, in *Tissue Oxygen Deprivation*, G. G. Haddad and G. Lister, Eds. (Dekker, New York, 1996), pp. 433–477.
15. D. Gozal *et al.*, *Am. J. Respir. Crit. Care Med.* **155**, 1755 (1997).
16. J. Jerecic *et al.*, *Ann. N.Y. Acad. Sci.* **868**, 27 (1999).
17. D. L. Browne *et al.*, *Nature Genet.* **8**, 136 (1994).
18. J. P. Adelman, C. T. Bond, M. Pessia, J. Maylie, *Neuron* **15**, 1449 (1995).
19. S. M. Zuberi *et al.*, *Brain* **122**, 817 (1999).
20. B. C. Schroeder, C. Kubisch, V. Stein, T. J. Jentsch, *Nature* **396**, 687 (1998).
21. C. Biervert *et al.*, *Science* **279**, 403 (1998).
22. J. M. Ramirez and D. W. Richter, *Curr. Opin. Neurobiol.* **6**, 817 (1996).
23. K. Nishimori *et al.*, *Proc. Natl. Acad. Sci. U.S.A.* **93**, 11699 (1996).
24. J. F. Renaud *et al.*, *Nature* **319**, 678 (1986).
25. D. Pribnow and J. P. Adelman, *Curr. Res. Ion Channel Modulators* **3**, 221 (1999).
26. M. I. Behrens, P. Jalil, A. Serani, F. Vergara, O. Alvarez, *Muscle Nerve* **17**, 1264 (1994).
27. P. Dufour *et al.*, *Eur. J. Obstet. Gynecol. Reprod. Biol.* **72**, 159 (1997).
28. S. Rudnik-Schoneborn, G. A. Nicholson, G. Morgan, D. Rohrig, K. Zerres, *Am. J. Med. Genet.* **80**, 314 (1998).
29. K. G. Chandy *et al.*, *Mol. Psychiatry* **3**, 32 (1998).
30. A. L. Blatz and K. L. Magleby, *Nature* **323**, 718 (1986).
31. P. A. Furth *et al.*, *Proc. Natl. Acad. Sci. U.S.A.* **91**, 9302 (1994).
32. N. Sternberg and D. Hamilton, *J. Mol. Biol.* **150**, 467 (1981).
33. E. Y. Chen *et al.*, *Genomics* **4**, 479 (1989).

34. We thank H. Bujard for graciously providing elements of the tTA system. This work was supported by grants from the NIH, the Muscular Dystrophy Association, the Human Frontiers of Science Program, and ICAgen (to J.P.A. and J.M.) and by the Volkswagen Foundation and the Bristol-Myers Squibb Foundation (to P.H.S.).

4 January 2000; accepted 21 July 2000

Interhemispheric Asymmetries of the Modular Structure in Human Temporal Cortex

Ralf A. W. Galuske,[1]* Wolfgang Schlote,[2] Hansjürgen Bratzke,[3] Wolf Singer[1]

Language-relevant processing of auditory signals is lateralized and involves the posterior part of Brodmann area 22. We found that the functional lateralization in this area was accompanied by interhemispheric differences in the organization of the intrinsic microcircuitry. Neuronal tract tracing revealed a modular network of long-range intrinsic connections linking regularly spaced clusters of neurons. Although the cluster diameter was similar in both hemispheres, their spacing was about 20 percent larger in the left hemisphere. Assuming similar relations between functional and anatomical architecture as in visual cortex, the present data suggest that more functionally distinct columnar systems are included per surface unit in the left than in the right area 22.

Neuropsychological, electrophysiological, and noninvasive imaging studies indicate that language comprehension and production are accompanied by activation of certain cortical areas. Several of these areas are activated only unilaterally in the dominant hemisphere (*1*, *2*). One of the regions exhibiting robust unilateral activation during processing of language-related signals is located in the posterior part of the first temporal gyrus and the posterior temporal plane (Fig. 1A) (*3*–*6*). This region corresponds to a discrete cytoarchitectonical entity, the posterior part of area 22 in the Brodmann classification (*7*), or to

Table 1. Interpatch distances and patch sizes in area 22.

Patient	Distance (left/right)	*n*	*P**	Size (left/right)	*n*	*P**
M1	1450 μm	10		856 μm	10	
	1236 μm	16	0.0114	844 μm	26	0.7
M2	1432 μm	22		689 μm	24	
	1099 μm	27	<0.0001	616 μm	36	0.015
M3	1463 μm	20		728 μm	24	
	1234 μm	23	0.0402	707 μm	23	0.49
M4	1544 μm	43		746 μm	58	
	1303 μm	34	0.0016	734 μm	42	0.64
M8	1630 μm	28		823 μm	28	
	1464 μm	30	0.0203	802 μm	27	0.39
M9	1149 μm	45		572 μm	48	
	1022 μm	23	0.0294	558 μm	26	0.41
M11	1370 μm	44	0.0341	589 μm	47	0.0797
	1207 μm	19		640 μm	19	

**P* values arising from Mann-Whitney *U* test.

area TA1 after von Economo and Koskinas (*8*) and is distinguishable in both hemispheres on the basis of common cytoarchitectonic features. However, the temporal plane [(*9*), but see (*10*)], in particular, area 22 (*11*), is significantly larger, and cell size and density are superior in the dominant hemisphere (*12*, *13*). In the dominant hemisphere, area 22 is involved in word detection and generation (*3*–*6*), which have been attributed to its ability to process rapid frequency changes (*14*, *15*), whereas the homolog area in the nondominant hemisphere appears to be specialized in the discrimination of melody, pitch, and sound intensity (*16*, *17*).

The low spatial resolution of noninvasive methods prevents the analysis of local processing architectures in the human brain. However, certain aspects of microcircuitry can be studied postmortem with neuronal tracing techniques. In the visual cortex, close relations could be established between the layout of long-range intrinsic connections and the functional organization of cortical modules. These connections exhibit a high degree of topological specificity (*18*, *19*) and reciprocally link discrete clusters of supragranular pyramidal cells that are spaced at regular intervals (*20*, *21*) and share similar functional properties (*22*–*24*).

We examined the layout of long-range intrinsic connections in the posterior part of area 22 (Fig. 1A) of both hemispheres using postmortem implantation of carbocyanine dyes (*25*–*27*). To establish the extent to which interhemispheric structural differences already exist on the level of primary sensory areas, we also examined intrinsic connections in the primary auditory cortex (area 41, Fig. 1A) of a limited sample of subjects.

In posterior area 22, we found a dense plexus of tangential connections (Fig. 1D) bridging distances of up to 7 mm. Stained structures consisted of anterogradely labeled axons (Fig. 1E) and retrogradely labeled neurons (Fig. 1, B and C). Most of these neurons, especially at distances >3 mm from the site of dye implantation, were concentrated in supragranular layers and exhibited the morphological features of pyramidal cells (Fig. 1, B and C). Layer IV contained only very few labeled axons and retrogradely stained neurons. A small number of long-range axons and retrogradely labeled cells were present in layer V, and the latter were in register with labeled neurons in supragranular layers. As in the visual cortex, retrogradely labeled cells and anterogradely stained axonal terminal arbors tended to be superimposed and to form regularly spaced clusters around the injection site (Fig. 1, C to E). For interhemispheric comparison of this architectural feature, we quantified the size of the labeled clusters and their spacing (*27*). The size of the labeled clusters was similar in both hemispheres (Table 1 and Fig. 2C). However, the center-to-center distance of the clusters was significantly larger in the left hemisphere in all seven subjects (Table 1 and Fig. 2C). The

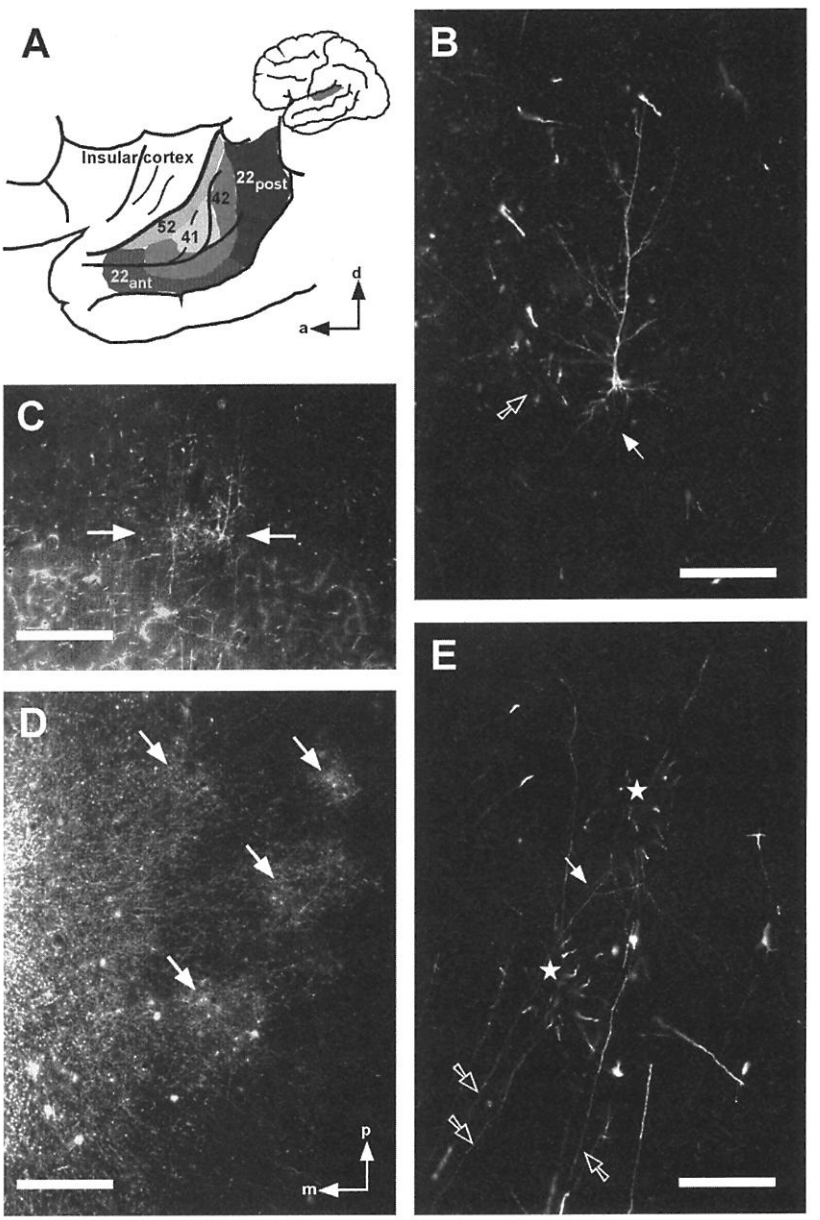

Fig. 1. (**A**) Cytoarchitectonic subdivision of the upper portion of the temporal lobe (see shaded area in the inset) according to the classification of Brodmann (*7*). This parcellization is closely related to the classification of von Economo and Koskinas (*8*), with area 41 corresponding to TC, area 52 to TD, area 42 to TB, the posterior (post) portion of area 22 to TA_1, and the anterior (ant) portion of area 22 to TA_2. a, anterior; p, posterior. (**B** to **E**) Patterns of postmortem DiI labeling in area 22 of the human temporal cortex. (B) Retrogradely labeled supragranular pyramidal neuron, about 5 mm from the dye crystal. Filled arrow, axon; open arrow, horizontal axon collateral. Scale bar, 125 μm. (C) Cluster of retrogradely DiA-labeled neurons (between the arrows) in the supragranular layers about 4 mm from the dye crystal. Scale bar, 250 μm. (D) Clusters of retrogradely labeled cells and anterogradely labeled axon terminals (arrows) in a tangential section through supragranular layers of left area 22. The dye crystal was about 1.5 mm beyond the left edge of the micrograph. Scale bar, 1 mm. m, medial; p, posterior. (E) DiI-labeled axons (open arrows) converging onto the same spot in a tangential section through supragranular cortical layers about 4.5 mm from the dye crystal. Filled arrow, terminal branching of one of the axons; asterisks, dendrites of two retrogradely labeled neurons. Scale bar, 100 μm.

[1]Department of Neurophysiology, Max-Planck-Institute for Brain Research, Deutschordenstrasse 46, 60528 Frankfurt a.M., Germany. [2]Neurological Institute (Edinger Institute), University of Frankfurt Medical School, Deutschordenstrasse 46, 60528 Frankfurt a.M., Germany. [3]Institute of Forensic Medicine, University of Frankfurt Medical School, Kennedyallee 104, 60596 Frankfurt a.M., Germany.

*To whom correspondence should be addressed: E-mail: galuske@mpih-frankfurt.mpg.de

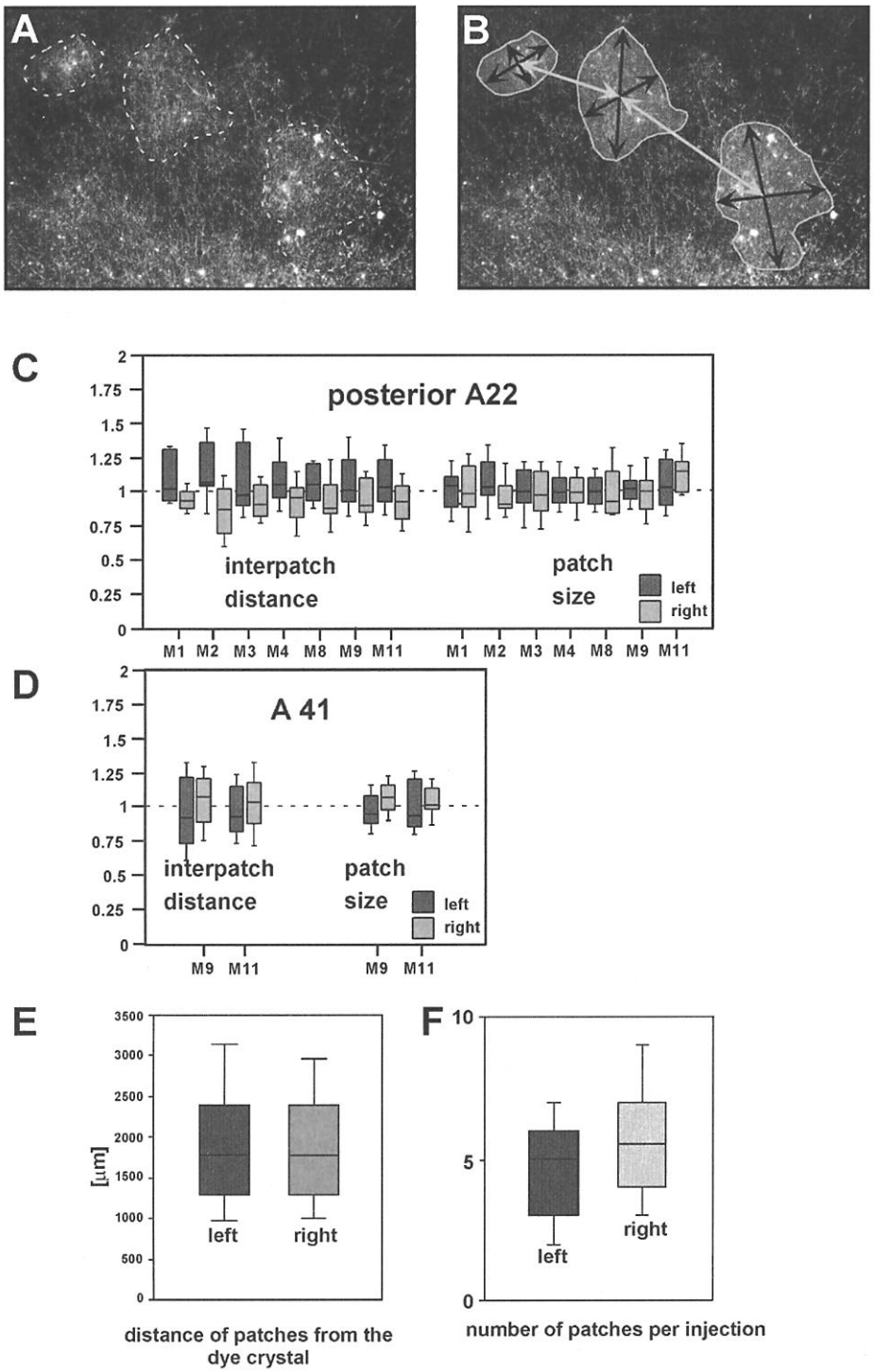

Fig. 2. (**A**) Same horizontal section as in Fig. 1D, with dashed outlines demarcating patches. (**B**) Same as (A), with lines indicating measured variables. Black arrows, patch diameters; gray arrows, interpatch distances. (**C**) Box plots of interpatch distances and patch sizes (ordinate) in the posterior part of area 22. Boxes represent the 25th and the 75th percentile; horizontal lines indicate the 10th and 90th percentile. Measurements from the same cases are grouped together; light gray boxes indicate data from left hemispheres, and dark gray boxes indicate data from right hemispheres. Data are normalized to the respective mean value in each brain. (**D**) Box plots of the interpatch distances and patch sizes in the primary auditory cortex (area 41). Conventions as in (C). (**E**) Box plots of distances between patches and injection site in area 22. (**F**) Box plots of the number of labeled clusters per dye injection in area 22.

Table 2. Interpatch distances and patch sizes in the primary auditory cortex.

Patient	Distance (left/right)	*n*	*P**	Size	*n*	*P**
M9	867 µm	30		394 µm	30	
	952 µm	52	0.1037	420 µm	54	0.04
M11	874 µm	36		418 µm	42	
	913 µm	37	0.4256	432 µm	37	0.203

*P values arising from Mann-Whitney U test.

magnitude of this difference ranged from 12 to 30% (Table 1). Comparative data from the primary auditory cortex in two of the subjects, which both showed a significant asymmetry in posterior area 22, did not reveal interhemispheric differences in spacing, suggesting that the observed differences in posterior area 22 are not reflecting a general interhemispheric asymmetry of microcircuitry in the temporal lobe (Table 2 and Fig. 2D). However, this issue needs further investigation by analysis of other components of the central auditory system.

Clustering could be a reflection of interdigitating subsystems of selectively interconnected columns or of a single system of discrete, grid-like connections. We implanted both dyes, DiI and DiA, in the same block of tissue (n = 10) at distances ranging from 1.5 to 3 mm. Each crystal labeled several clusters of neurons over a distance of up to 5 mm from the injection site. In most cases (n = 8), clusters labeled by different dyes were nonoverlapping and interleaved (Fig. 3A). In only two cases, a few of the clusters overlapped (Fig. 3B). The overlap included the complete area of single clusters, indicating that the two injections labeled the same connectivity system. This suggests the first scenario, i.e., interdigitating subsystems of selectively interconnected columns. Because cluster size was similar in the two hemispheres, the wider spacing implies that more subsystems can be included per surface unit in the left than in the right area 22. This interpretation is supported by the interhemispheric comparison of the number of clusters labeled by a single dye implantation and the distance of clusters from the implantation site (Fig. 2, E and F). The average distance of the clusters from the implantation site was similar in both hemispheres (Fig. 2E). Accordingly, the number of labeled clusters per injection was slightly smaller in the left than in the right hemisphere (Fig. 2F), suggesting that left area 22 contains fewer elements of an individual connectivity system per unit area.

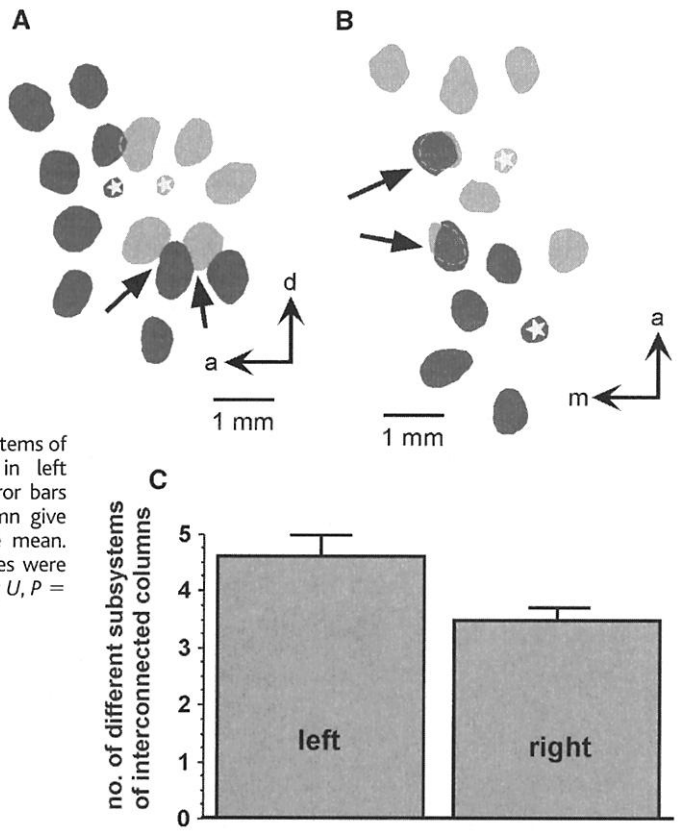

Fig. 3. (**A** and **B**) Camera lucida drawings of the patchy patterns of long-range intrinsic connections in tangential sections through area 22 after simultaneous injection of DiI and DiA. Dark gray, DiI; light gray, DiA; asterisks, implantation sites. m, medial; a, anterior; d, dorsal. (A) Pattern with interdigitating patches (arrows). (B) Pattern with two double-labeled patches (arrows). (**C**) Estimation of the number of different subsystems of interconnected columns in left and right area 22. The error bars on the top of each column give the standard error of the mean. Interhemispheric differences were significant (Mann-Whitney U, $P = 0.01$).

Calculations based on the measured cluster size and spacing suggest that the left area 22 can contain about 30% more distinct subsystems within the same volume of tissue (Fig. 3C). Because area 22 is larger in the dominant than in the nondominant hemisphere (*11*), interdigitation of more columnar subsystems can be achieved without reducing the number of columns constituting a particular subsystem. Thus, if these subsystems are tuned to different features, as in the visual cortex, more feature domains could be represented in the left than in the right area 22 without reduction of the number of neurons devoted to a particular feature. This, then, is likely to permit a more fine-grained analysis of feature domains, and we propose that this is related to special functions of auditory processing such as are required, e.g., for the analysis of speech.

An increase in cluster spacing has also been noted in higher areas of the visual cortex, and it has been proposed that this might reflect the need to represent more complex feature constellations in higher areas (*28*).

Neuropsychological studies in patients with temporal lesions or callosotomy suggest that the nondominant hemisphere has a limited capacity to handle language and to substitute for the loss or inaccessibility of the language areas in the dominant hemisphere (*29*). We propose that this limitation may be related to the different connectivity patterns identified in the present study.

Because early lesions in language areas of the dominant hemisphere can be compensated by the nondominant hemisphere (*30*), it is conceivable that the observed interhemispheric differences in the layout of intrinsic connections are at least in part due to use-dependent modifications of circuitry during early development. Future studies will have to determine the exact time course of postnatal maturation of this connection system.

References and Notes

1. M. E. Raichle, *Annu. Rev. Psychol.* **45,** 333 (1994).
2. J. R. Binder *et al.*, *J. Neurosci.* **17**, 353 (1997).
3. S. E. Petersen, P. T. Fox, M. I. Posner, M. Mintun, M. E. Raichle, *Nature* **331**, 585 (1988).
4. D. Howard *et al.*, *Brain* **115**, 1769 (1992).
5. J. F. Demonet, R. Wise, R. S. J. Frackowiak, *Hum. Brain Mapp.* **1**, 39 (1993).
6. J. A. Fiez, M. E. Raichle, D. A. Balota, P. Tallal, S. E. Petersen, *Cereb. Cortex* **6**, 1 (1996).
7. K. Brodmann, *Vergleichende Lokalisationslehre der Großhirnrinde* (Barth, Leipzig, Germany, 1909).
8. C. v. Economo and G. N. Koskinas, *Die Cytoarchitektonik der Hirnrinde des erwachsenen Menschen* (Springer-Verlag, Berlin, 1925).
9. N. Geschwind and W. Levitsky, *Science* **161**, 186 (1968).
10. W. C. Loftus *et al.*, *Cereb. Cortex* **3**, 348 (1993).
11. A. Galaburda, F. Sanides, N. Geschwind, *Arch. Neurol.* **35**, 812 (1978).
12. H. L. Seldon, *Brain Res.* **229**, 277 (1981).
13. J. J. Hutsler and M. S. Gazzaniga, *Cereb. Cortex* **6**, 260 (1996).
14. J. Schwartz and P. Tallal, *Science* **207**, 1380 (1980).
15. P. Belin, M. Zilbovicius, S. Crozier, L. Thivard, A. Fontaine, *J. Cogn. Neurosci.* **10**, 536 (1998).
16. R. J. Zattore, A. C. Evans, E. J. Meyer, *J. Neurosci.* **14**, 1908 (1994).
17. P. Belin *et al.*, *J. Neurosci.* **18**, 6388 (1998).
18. K. S. Rockland and J. S. Lund, *Science* **215**, 1532 (1982).
19. J. S. Lund, T. Yoshioka, J. B. Levitt, *Cereb. Cortex* **3**, 148 (1993).
20. C. D. Gilbert and T. N. Wiesel, *J. Neurosci.* **3**, 1116 (1983).
21. Z. F. Kisvarday and U. T. Eysel, *Neuroscience* **46**, 275 (1992).
22. D. Ts'o, C. D. Gilbert, T. N. Wiesel, *J. Neurosci.* **6**, 1160 (1986).
23. C. D. Gilbert and T. N. Wiesel, *J. Neurosci.* **9**, 2432 (1989).
24. K. E. Schmidt, D.-S. Kim, W. Singer, T. Bonhoeffer, S. Löwel, *J. Neurosci.* **17**, 5480 (1997).
25. A. Burkhalter, K. L. Bernardo, V. Charles, *J. Neurosci.* **13**, 1916 (1993).
26. R. A. W. Galuske and W. Singer, *Cereb. Cortex* **6**, 417 (1996).
27. We examined brains of seven subjects who to the best of our knowledge were free of neurological disorders. Six of the subjects were males (34, 41, 51, 52, 53, and 73 years old) and one was an 82-year-old female. After a postmortem delay of 18 to 24 hours, blocks of tissue containing area 22 were prepared (Fig. 1A) and fixated for 48 hours in a solution containing 2.6% paraformaldehyde (PA), 0.8% iodacetic acid, 0.8% sodiumperiodate, and 0.1 M D-L-lysine in 0.1 M phosphate buffer at pH 7.4. Subsequently, blocks were washed in phosphate buffer, and crystals of DiI and DiA, about 400 μm in diameter, were implanted into the cortex. Usually three to four blocks of area 22 of each hemisphere were prepared and implanted. To estimate the lateral extent of the connections, we only implanted one crystal of each dye per block. The tissue was stored for 4 to 6 months in 2% PA in phosphate buffer at pH 7.4 in the dark at 37°C. Vibratome sections were then cut at a thickness of 70 μm, either parallel or perpendicular to the pial surface, to determine the laminar as well as the tangential organization of the intrinsic axon systems. The areal boundaries were determined in cresyl violet–stained sections according to the criteria of von Economo and Koskinas (*8*) (Fig. 1A). The geometrical parameters of the layout of long-range intrinsic connections were analyzed on camera lucida drawings of sections cut parallel either to the surface of the temporal plane or parallel to the lateral surface of the first temporal gyrus at ×50 magnification, as exemplified in Fig. 2, A and B. Measurements were restricted to regions of sections that were parallel to the cortical lamination. Labeled zones were classified as patches if well-demarcated clusters of anterogradely labeled terminal arbors contained also retrogradely labeled cells. Usually the patches were easily discernable from the background as the coincidence of dendrites and axon terminal fields produced a strong contrast. The position of the patches in individual sections was confirmed by the continuity of the patches into neighboring sections. To avoid any bias, we did measurements blindly on coded sections. Patch diameter was determined from the mean of the respective longest and shortest diameter. The crossing points of the two diameters were taken as patch center, and interpatch distances were measured between nearest neighbors (Fig. 2B). For inter-individual comparison, the distributions obtained in each subject were normalized to the respective mean values of patch size and interpatch distance in each brain. Calculations on the number of different patch systems, as indicated in Fig. 3C, are based on the assumption that the patches are round and equally spaced according to the parameters measured in the respective hemispheres in the different subjects.
28. Y. Amir, M. Harel, R. Malach, *J. Comp. Neurol.* **334**, 19 (1993).
29. K. Baynes, *J. Cogn. Neurosci.* **2**, 159 (1990).
30. A. Smith and O. Sugar, *Neurology* **25**, 813 (1975).

31. We thank S. Schwegmann, P. Janson, E. Raulfs, M. Sum, and W. Hofer for excellent technical assistance; R. Ruhl for her qualified help during the preparation of the illustrations; and D.-S. Kim and R. Goebel for helpful comments and suggestions on the manuscript.

16 May 2000; accepted 11 July 2000